ADVANCED MATERIALS

DOI: 10.1002/adma.200602846

Enhanced Stiffness of Amorphous Polymer Surfaces under Confinement of Localized Contact Loads**

By *Catherine A. Tweedie*, *Georgios Constantinides*, *Karl E. Lehman*, *Donald J. Brill*, *Gregory S. Blackman*, and *Krystyn J. Van Vliet**

Although there is an increasing appreciation that physical properties of amorphous (glassy) polymer surfaces and interfaces can differ substantially from those of the bulk, the mechanisms and implications for mechanical performance of thin films, surfaces of bulk polymers, and nanocomposites are unclear. For example, several natural and synthetic nanocomposites exhibit markedly enhanced stiffness and strength that cannot be explained via two-phase composite rules-of-mixtures. Here we apply recent advances in contact deformation to determine the apparent elastic (or storage) moduli over 5 to 200 nanometers from the free surface of amorphous polystyrene, poly(methyl methacrylate), and polycarbonate. We observe that the apparent stiffness of the surface under contact can exceed that of the bulk by up to 200%, independent of processing scheme, macromolecular structural characteristics, and relative humidity. We attribute this enhanced apparent stiffness at the surface to the contact stress-induced formation of a mechanically confined phase at the probe-polymer interface. These observations are consistent with the increased macromolecular mobility of glassy polymer free surfaces, and relate directly to the material physics of the interphase in synthetic and biological polymer nanocomposites.

Most experimental investigations of amorphous polymer surfaces have focused on thermally activated behavior such as the glass transition temperature T_g[1–3] and structural relaxation.[4,5] However, few overarching conclusions exist regarding surface and interface properties,[6] in large part because experimental and sample preparation capabilities have not yet been optimized for the nanometer-length scales over which these surface-specific phenomena are observed. There are two generally accepted conclusions regarding amorphous polymer surface behavior: that T_g is a function of polymer film thickness t_f for $t_f < 100$ nm, and that the magnitude and direction of the T_g shift depends on the polymer and/or substrate[7]. For example, the T_g of amorphous polystyrene (PS) films has been found to be depressed by 35°C in spin-coated films of $t_f < 20$ nm on Si substrates[1] and by 70°C for free standing films of $t_f < 30$ nm,[2] while amorphous poly(2-vinylpyridine) has demonstrated a 35°C elevation in T_g for $t_f = 10$ nm that is attributed to secondary bonding with the Si substrate.[8]

Here, we sought to consider the consequences of such a physical property variation on the resistance of amorphous polymer surfaces to localized contact deformation. Depression of T_g in polymers such as PS and PMMA suggests that, over distances < 100 nm from the free surface of these so-called glassy polymers, the macromolecular chains are more mobile than those located within the bulk. This conceptualization is consistent with computational simulations of molecular mobility of free surfaces and confined volumes,[9–11] as well as recent experimental observations for PS thin films of $t_f < 40$ nm, including broadened structural relaxation times[4] and decreased elastic moduli inferred from film buckling.[12] Such elastic instabilities are important to defining the mechanical behavior of polymer free surfaces; however, the response of mechanically loaded or confined surfaces may differ from that inferred via non-contact experiments, especially for polymers.[13,14] In fact, several recent contact-based studies of polymer surfaces[15–17] have indicated elastic properties differing from that of the bulk, but both the trends and mechanisms remain unclear. For example, several studies have indicated significant increases in elastic or storage moduli E or E' of copolymer, semicrystalline and amorphous polymer surfaces for indentation depths $h_c < 50$ nm,[15,16,18,19] but may be attributable at least in part to microstructural inhomogeneities on this length scale or to experimental uncertainties such as incomplete knowledge of the nanoscale probe geometry.[14] In contrast, contact-based rheological studies in other polymers tested[20] or heated[21] above bulk T_g have not identified differences in stress relaxation[20] or JKR adhesion-inferred elastic moduli[21] as a function of distance from the free surface. Here, we propose that the depressed T_g of amorphous polymer surfaces can result in a mechanically distinct region at the probe-polymer interface, resulting in an apparent stiffness that exceeds the elastic response of the bulk polymer.

[*] Prof. K. J. Van Vliet, C. A. Tweedie, G. Constantinides
Department of Materials Science and Engineering
Massachusetts Institute of Technology
Cambridge, MA 02139 (USA)
E-mail: krystyn@mit.edu
Dr. G. S. Blackman, K. E. Lehman, D. J. Brill
DuPont Central Research & Development
E356, Wilmington, DE 19880 (USA)

[**] We gratefully acknowledge Y. Brun, K. Sharp, M. Wetzel, and B. Bennett for helping to synthesize and characterize these samples. We especially appreciate discussion with A.M. Mayes and M.F. Rubner, and acknowledge use of the Shared Experimental Facilities supported by the MRSEC Program of the National Science Foundation (DMR 02-13282). We thank the DuPont-MIT Alliance (KJVV, GC, and CAT) and the National Science Foundation Graduate Fellowship program (CAT) for support of this research. Supporting Information is available online from Wiley InterScience or from the author.

In this study, we measured the apparent stiffness of several amorphous polymer surfaces at room temperature, in response to five maximum indentation loads imposed through two well-characterized conospherical diamond probes of approximate radii R = 500 nm and 9 μm (Fig. 1a). These maximum loads corresponded to indentation contact depths h_c ranging 5 nm to >100 nm from the free surface (Fig. 1b). To infer the elastic response of the polymer from this contact loading as an apparent elastic modulus or stiffness E_a, we designed these experiments to minimize viscous contributions[22] and account for geometric non-ideality of the spherical probes;[23] consideration of these and other potential artefacts in nanoscale contact mechanics are discussed in Experimental. We intentionally chose to consider an ensemble of well-controlled, amorphous polymers including PS and PMMA, as the physical and mechanical properties (of the bulk and of thin films) have been determined by us and others using several complementary approaches.[2–4,7,12,13,17,24–28] As described below, in all of these polymers that were considered over a range of processing, loading, and environmental conditions, we consistently observed an increase in apparent stiffness E_a of up to 200% measured close to the surface, relative to that 100s of nanometers from the surface; Fig. 1c illustrates this trend for compression-molded PS. At depths > 50 nm, E_a tended toward the elastic moduli of the bulk polymer as measured by indentation[29] or by uniaxial compression; see Experimental. We assert that this enhanced apparent stiffness near the surface is the result of an interface formed at the contact surface confined between the polymer and the diamond probe – a region of unique structural and/or physical properties termed the interphase.[30,31] As this phenomenon would have significant implications regarding enhanced mechanical stiffness of nanocomposites and other material systems that are confined or mechanically loaded at the nanoscale, we explored this apparent stiffness as a function of processing and thermal history, polymer structure (molecular weight, monomer structure, and persistence length), relative humidity, and experimental parameters such as probe radius.

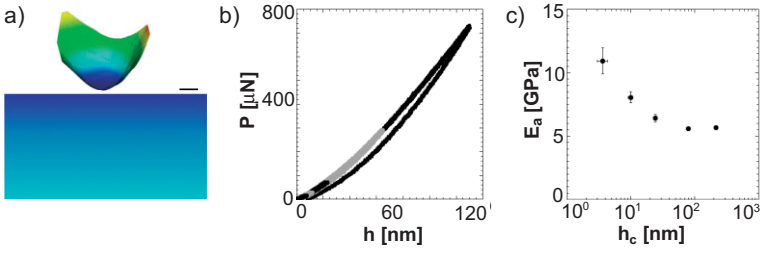

Figure 1. Apparent stiffness of polymer surfaces under contact. a) Schematic of a nanoindentation probe (image reconstructed from atomic force microscopy, scalebar = 500 nm) approaching an amorphous polymer surface with higher molecular mobility over the first ~40 nm from the surface. b) Representative indentation load-displacement curves to five maximum loads *P* corresponding to a range of indentation depths *h* are displayed alternately in black and grey. c) The indentation elastic modulus *E* increases with decreasing indentation depth h_c in compression molded polystyrene, molecular weight M_w = 12 kg/mol. Error bars represent one standard deviation and may be smaller than the symbol.

To consider whether this surface stiffening was a function of structural attributes of these amorphous homopolymers, we first varied the molecular weight of PS by over an order of magnitude. Nanoindentation of two compression-molded PS samples of weight-average molecular weight M_w = 12.45 kg/mol (PS-12k), near the entanglement molecular weight of ~13 kg/mol[12] for PS, and M_w = 194 kg/mol (PS-194k) quantitatively demonstrated the same stiffening at ~5 nm from the free surface (Fig. 2a), indicating that this stiffening mechanism is independent of M_w, macromolecule radius of gyration, or chain-end density at the surface, at least over this range of M_w. In addition, we considered bulk amorphous polymers with significantly different persistence lengths to further probe the effects of monomer structure on this apparent stiffening. Persistence length *b*, the length scale over which a polymer chain is effectively rigid,[32] was compared for three amorphous polymers: polycarbonate (PC-18k; b_{PC} = 3 nm[33]), PMMA (PM-15k; b_{PM} = 1.3 nm[34]), and PS-12k (b_{PS} = 0.9 nm[32]), over the same range of contact depths, 5 nm < h_c < 200 nm. Although E_a was greatest at the surface for all three polymers, the extent to which the PM-15k surface stiffened was significantly less than that of PS-12k or PC-18k,[55] despite the fact that the persistence length of PMMA is bounded by that of PS and PC. As discussed below, this is consistent with the observation that the depression of T_g observed for PMMA is not as pronounced as in PS of the same molecular weight ranges.[35] Note that the apparent stiffness in Fig. 2a is normalized for all polymers only for visual clarity, and that E_a at h_c >100 nm was consistent with that of macroscopic volumes for all polymers.[55] Thus, we concluded that molecular weight and persistence length do not strongly contribute to this apparent stiffening of the contact loaded surface.

To consider whether this apparent stiffness could be attributed to processing-dependent changes in structural, physical, and mechanical properties at the surface[36], we employed four different processing and thermal history routes (compression molding (CM), injection molding (IM), spin coating (SC) and annealing after spin coating (SC-A)) for PS and PMMA. These routes were modified to minimize surface roughness to < 1 nm, as confirmed by atomic force microscopy. As shown in Fig. 2b for the case of PS-12k, all processing routes resulted in identical increases in E_a at the surface over 5 ≤ h_c ≤ 200 nm. For contact depths greater than 20 nm, spin-coated films of ~1 μm thickness appeared stiffer than the compression- or injection-molded samples of millimeter-scale thickness. We confirmed through finite-element simulation of this experimental system[54] that this transition is expected at such depths due to the mechanical contribution of the underlying, stiff Si substrate. As thin films formed from a solvent and bulk discs formed from a confined melt exhibited the same apparent stiffness at the surface, we concluded that this effect cannot be attributed to processing-induced artefacts at the surface.

ADVANCED MATERIALS

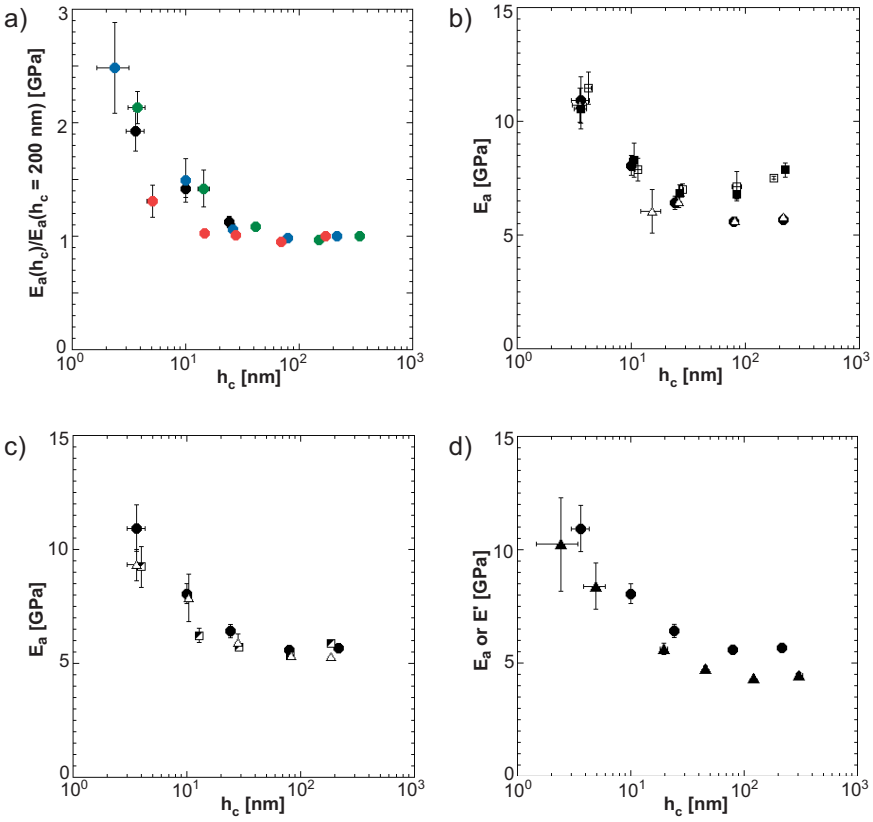

Figure 2. Dependence of apparent stiffness under contact loading on polymer processing, structure, and physical environment. a) Compression molded polystyrene (PS) samples with M_w = 12 kg/mol (black) and M_w = 197 kg/mol (blue) as well as polycarbonate (PC) with M_w = 18 kg/mol (green) exhibit statistically equivalent stiffening trends toward the surface, while poly(methyl methacrylate), PMMA with M_w = 15 kg/mol stiffened at the surface to a lesser extent (red). Data are normalized for each material with respect to E_a measured at $h_c \sim 200$ nm for clarity, as the plateau stiffness of PMMA overlaps with the decreasing stiffness trends of PS and PC. b) Apparent stiffness E_a increases with decreasing contact depth h_c in PS (molecular weight M_w = 12 kg/mol) for compression molded (●), injection molded (△), spin-coated (□), and annealed/spin-coated (■) PS. Both spin-coated samples appear stiffer for $h_c \geq 20$ nm than for other processing routes because of the Si substrate contribution to the mechanical response. c) There is no effect of relative humidity (% RH) on the extent of stiffening at the surface of compression molded PS: 42% RH before oven drying (●), 10% RH after oven drying (△), 42% RH after oven drying (half-filled square). d) Quasistatic nanoindentation (●) and nanoscale dynamic mechanical analysis at an oscillation frequency of 90 Hz (▲) of polystyrene (PS-12k) both demonstrate significant stiffening of the amorphous polymer surface for contact deformation experiments. Error bars represent one standard deviation and may be smaller than the symbol.

To consider whether ambient environmental effects such as relative humidity could induce such a significant mechanical changes at the polymer surface under contact, we evaluated the CM PS-12k surface as a function of % relative humidity (RH). As shown in Fig. 2c, this polymer demonstrated no statistical variation in E_a among experiments conducted at 42% RH (before and after drying the polymer for 2 h in a 105°C oven to exceed the boiling point of water) and those conducted within a 10% RH chamber (after drying the polymer). Although it would not be expected that a hydrophobic, amorphous polymer such as PS would be particularly susceptible to the presence of water at the surface, this experiment confirms this intuition over nanoscale distances from the PS free surface, where water meniscus formation[37a] or physical adhesion to the probe may be plausible. Data such as in Fig. 1b also demonstrate a lack of significant probe-surface adhesion force (< 0.3 μN for $h_c < 50$ nm). Further, for our probe radii R and apparent elastic moduli E, and the well-documented surface energy of these polymers γ, the Tabor parameter of adhesion $\mu(R, E, \gamma) < 2$ in all cases: neither JKR nor DMT theories of contact adhesion apply[37b,c]. Even in the case of strong JKR-type contact adhesion for elastomers such as poly(dimethoxysilane) or PDMS, it can be inferred from recent reports that elastic moduli extracted from indentation experiments on materials that exhibit measurable probe-surface adhesion forces ($E_{PDMS} \sim 2.9$ MPa)[37d] do not necessarily or significantly exceed that of uniaxial measurements on bulk forms of those same polymers (E_{PDMS} = 3.5 ± 0.2 MPa)[37e].

To consider whether this apparent stiffness under monotonic loading was representative of the storage component of a viscoelastic response, we employed nanoscale dynamic mechanical analysis (nano-DMA[38,39]) for the same probes and range of contact depths. As shown in Fig. 2d for the case of PS-12k, we observed quantitatively comparable increases in the apparent storage modulus obtained under oscillatory loading E' and apparent stiffness obtained under monotonic loading E_a. Importantly, DMA includes the viscous response of the polymer that is intentionally minimized in our evaluation of E_a. Nevertheless, over the range of accessible oscillation frequencies ranging from 10 to 250 Hz, E' at $h_c < 50$ nm from surface significantly exceeded that at $h_c > 100$ nm. Finally, none of the inorganic crystalline and amorphous materials (e.g., single crystal gold and borosilicate glass, Supp. Data Fig. 1) that were characterized over the same contact depths and range of experimental conditions exhibited an increase in elastic moduli near the free surface.

Observations of enhanced mechanical stiffness of these amorphous polymers over contact depths $h_c < 50$ nm may appear counter to that expected from a surface of increased molecular mobility. We posited that the marked stiffening of these polymer surfaces could be due to either a thin, mechanically stiff layer spanning the entire polymer surface, or to the formation of a mechanically distinct interfacial region induced

under the confined contact loading. Both scenarios can be considered via comparison of the mechanical responses obtained in compression-molded PS-12k for probes of radii differing by over an order of magnitude (R_{eff} = 487 nm and 8724 nm) over the same range of contact depths (5 nm < h_c < 200 nm). For a given contact depth, the larger probe will deform a larger volume of material that can be defined by the radius of contact at the surface a and the surface area of contact between the probe and the polymer SA_c. If a stiff surface layer exists, analytical models of bilayers under contact predict that the elastic response of this composite will be an analytical function of a, but will be independent of probe radius R. However, as shown in Fig. 3a, this is counter to what we observed: the apparent stiffness observed for two probe radii does not result in consistent predictions of the stiff-layer modulus E_1 or of the effective layer thickness t [56]. In contrast, the apparent stiffness observed with each probe scales with the contact surface area SA_c, as determined numerically from three-dimensional atomic force microscopy images of the actual probes to the measured contact depth h_c (Fig. 3b). This scaling strongly suggests the formation of a mechanically unique interphase induced at the region of the amorphous polymer surface in contact with the mechanical probe. (The timescale for this interphase formation is less than seconds, whereas the duration of contact shown in Figs. 1–2 is constrained by the requirements of elastic contact analysis[22] to be ~2 s; this trend in greater apparent stiffness at the surface is also quantitatively reproduced over a range of dynamic contact frequencies (e.g., Fig. 2d).)

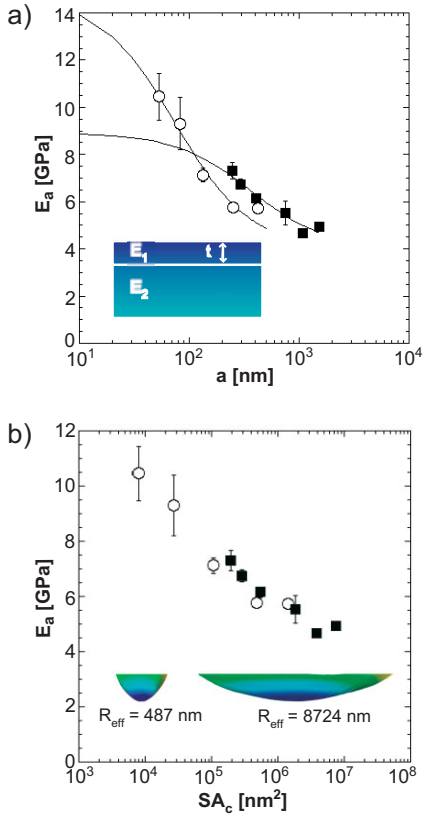

Figure 3. Possible mechanisms for mechanical stiffening of the contacted surface. a) The free surface could be a mechanically distinct, thin layer of thickness t that is stiffer than the underlying, glassy polymer ($E_1 > E_2$). Analytical theory for contact deformation of a bilayer mechanical model predicts that the composite elastic modulus $E(E_1, E_2, t)$ should vary as a function of contact radius a, but not of indenter radius R. Fits of this model (lines) to experimental data obtained with two probes of effective radii R_{eff} = 487 nm (○) and R_{eff} = 8724 nm (■) for polystyrene (PS-12k) do not coincide and thus do not support this model. b) A mechanically distinct phase could be formed in the material immediately adjacent to the probe surface, scaling with the surface area of contact SA_c for any probe radius R. These data show that E_a increases with decreasing surface area of contact SA_c for these probes, consistent with the formation of an interface at the region defined by probe-surface contact. Error bars represent one standard deviation and may be smaller than the symbol.

A range of recent experiments in PS supports this interpretation of a mechanically unique, induced interface during contact deformation of these surfaces. In particular, three distinct observations should be considered. First, although not all polymer free surfaces exhibit a depressed glass transition temperature,[25] a significant depression of T_g (30 K to 70 K for t_f ~ 10 nm) from the bulk value is consistently reported for PS thin films, both those adhered to substrata[1,3] and freestanding,[2, 27] and over a range of molecular weights. Recent work by Torkelson et al. has demonstrated the equivalence of T_g depression, indicative of molecular mobility, at the surface of "bulk" polymers (films of at least μm-scale thickness such as those we consider here) and at the surface of thin films (for t_f > 30 nm). PS films of t_f < 30 nm also exhibited depressed T_g, but no through-thickness gradient in this depression[1, 40]. Second, O'Connell and McKenna found this same magnitude of T_g depression (40 K) in free standing PS films of t_f ~ 20 nm, and further reported that PS films tested at elevated temperatures in the rubbery state exhibited a film thickness-dependent decrease in rubbery creep compliance. This decreased compliance corresponded to an increase in effective stiffness of the rubbery state from 10^6 Pa to 10^8 Pa as film thickness was decreased to t_f ~13 nm.[26] Third, Stafford et al. recently applied non-contact elastic buckling[27] to determine E_a of PS films on poly(dimethylsiloxane) at room temperature, and found an order of magnitude decrease in E_a of the PS films, from 10^9 Pa to 10^8 Pa as t_f approached 5 nm. To summarize these observations in the archetypal amorphous polymer PS: as film thickness or distance from the surface of observation decreases below ~30 nm, the T_g of both films and free surfaces decreases significantly, the apparent stiffness of the rubbery state increases by two orders of magnitude, and the apparent stiffness as measured by elastic buckling decreases by an order of magnitude.

One possible interpretation that reconciles these observations and is supported by our own findings is that contact loading creates an interfacial region of confined molecular motion and elevated T_g with respect to the uncontacted surface. Extrapolation of reported T_g (t_f) for PS[1] indicates that the T_g at a distance 5 nm from the polymer free surface is ~20°C below room temperature. This suggests that free surfaces and films explored over this length scale at room temperature are effectively in the rubbery regime, which is consis-

ADVANCED MATERIALS

tent with the ~0.1 GPa apparent stiffness observed via non-contact creep[26] and buckling[12] of PS films. However, upon contact with another surface such as the spherical diamond probes used in our experiments, this highly mobile region existing within 5 nm of PS free surfaces has the potential for significantly enhanced intermolecular interactions at the geometrically confined interface induced by the indenter probe[41]. Mechanical loading at this interface induces hydrostatic stress beneath the probe, which is well established to increase T_g by 0.3°C/MPa (for PS and PMMA[6,42]) to 0.4°C/MPa (for PC[43]). For the range of contact pressures in our experiments on these polymers, the hydrostatic stress beneath the spherical probes ranged from 250 to 400 MPa. In contrast to contact experiments on polystyrene in which no external force was applied,[44,45] these hydrostatic pressures indicate an increase in T_g of approximately 50°C – 120°C, which would shift the T_g of this region well above room temperature.

In other words, the uncontacted polymer surface may exhibit T_g near or above room temperature (and therefore an apparent stiffness of ~ 0.1 GPa corresponding to the rubbery state[12]), but the superposed contact stress shifts T_g at the probe/polymer interface upward to at least approach the stiffness of the bulk or glassy state. In addition to this mechanically imposed T_g shift, attraction toward and repulsion from the probe material could restrict molecular mobility in the confined region of mechanical contact adjacent to the probe, either via intermolecular interactions (enthalpic) or via stretching or alignment of macromolecular chains with respect to the probe surface (entropic via reduced conformations).[46] Significant variation of enthalpic interactions upon contact has been demonstrated by Roth et. al to decrease the molecular mobility of PS through variation of the contacting surface material, as well as in the development of nanoparticle-polymer matrix nanocomposites.[7,8,46,47].

Naturally, the relative volumetric proportion of this confined interfacial region will decrease as the total volume of strained polymer beneath the probe increases with increasing contact depth. As a result, the contribution of this interfacial region to the overall mechanical response will decrease to that of the bulk polymer with increasing contact depth, as observed here for depths $h_c > 200$ nm. This contribution will be diminished at a given contact depth for larger probe radii, which deform a larger total polymer volume at that depth. This is demonstrated by the comparison of apparent stiffness measured for a given contact depth for different contact surfaces areas (Fig. 3b). Thus, contact-based studies of polymer surfaces (tested or heated above bulk T_g) that employ probe radii or contact surface areas SA_c that exceed the range herein by orders of magnitude would not be expected to exhibit measurable differences in mechanical properties over tens of nanometers from the free surface.[20,21] For this same reason, the mechanical properties of the interphase region in nanoparticle-polymer nanocomposites will dominate the macroscopic mechanical response only when the volume fraction of the interphase is significant.

In summary, contact deformation to depths of $5 \text{ nm} < h_c < 200$ nm demonstrates as much as a 200% increase in the apparent stiffness of amorphous polymer surfaces, as compared to apparent elastic moduli measured for contact depths >200 nm from the free surface. For the three amorphous polymers considered, this increase in E_a is independent of processing, thermal history, macromolecular structural properties (molecular weight or persistence length), or relative humidity. The trend in apparent stiffness scales with the surface area of contact, and indicates that the polymer surface stiffening mechanism is related to the creation of a mechanically unique interfacial region between the probe and the polymer surface. These results provide the basis for isolating the effects of mechanical compression/confinement and of probe surface chemistry on the mechanical behaviour of polymer surfaces under localized contact. Our findings relate directly to the mechanical performance of polymers employed as protective barrier coatings. Further, this contact-induced stiffening may control deformation physics at the interphases formed in synthetic composites of amorphous polymer matrices and nanoscale particles,[7,47] as well as in biopolymeric surfaces and interfaces that define interphase cell rheology:[48] the unique mechanical properties of such synthetic and biological composites are often not explained by continuum rules of mixing two distinct phases.[30,46] It is plausible that mechanically distinct interphases induced upon contact loading between two phases (e.g., inorganic nanoparticles and an amorphous polymer matrix[49]) are responsible in part for the unexpected mechanical performance of such materials.

Experimental

Polymer Synthesis and Characterization: Polymer standards of polystyrene (PS) and poly(methyl methacrylate) (PMMA) were synthesized via anionic polymerization (Polymer Laboratories, Amherst, MA) and processed via three routes by DuPont (Wilmington, DE). Compression-molded (CM) samples were heated to ~150°C (above the polymer T_g) and compressed at loads of 0.3–0.5 tons (1 ton = 907.18 kg) between polished Al and an extremely smooth disk of float glass to yield samples of 1 mm thickness. Injection-molded (IM) samples were extruded above the melting temperature into a mold surface specially polished to reduce surface roughness, while spin-coated (SC) samples were spun onto Si wafers at 2000 RPM on a spin-coater (PM101D-1790, Headway, Garland, TX) using polymer solutions between 7.47 wt% and 22.4 wt% in 2-ethoxy ethanol for the PMMA, and methyl isobutyl for the PS. Profilometry (P10, KLA-Tencor, San Jose, CA) was used to measure the thickness of the SC PS-12k sample, yielding $t_f = 1140 \pm 13$ nm. The SC samples were annealed at T_g + 20°C to control for the effects of residual stress or retained solvent on the surface mechanics. The polycarbonate (PC) sample (Lexan, DuPont, Wilmington, DE) was injection molded into a smooth Al mold. All polymer sample surfaces were analyzed via optical profilometry and/or atomic force microscopy (AFM) imaging in tapping mode for surface roughness, and indicated root-mean-square roughness values of ≤ 1 nm for compression molded samples for which structural and environmental variables were considered, as well as spin-coated samples for which annealing was considered. These polymer surfaces were tested as processed, and any chemical or mechanical treatments post-processing were intentionally avoided. Single crystal, electropolished gold (Accumet Materials Co., Briarcliff Manor, NY) and amorphous

borosilicate (glass slide; VWR) served as non-polymeric control materials.

Weight-average molecular weight M_w was measured via gel permeation chromatography, while differential scanning calorimetry was used to determine the T_g of the two PS samples: M_w = 12 450 g/mol; PDI = 1.02; T_g = 96.9°C (or PS-12k) and M_w = 194 000 g/mol; PDI = 1.06; T_g = 106.9°C (or PS-194k), the PMMA sample: M_w = 14,920 g/mol; PDI = 1.04; T_g = 123.9°C (or PM-15k) and the PC sample: M_w = 18, 715 g/mol; PDI = 1.59; T_g = 145 °C (or PC-18k). In addition, the elastic modulus under compression was measured via a uniaxial load frame (Instron Inc., Canton, MA) for the compression molded PS-12k sample (E_c = 2.5 ± 0.4 GPa; n = 3), although elastic moduli extracted from micrometer-scale contact depths via (multiaxial) indentation loading of compression-molded PS are typically closer to 4 GPa [29].

Nanoindentation Experiments and Analysis: Sample surfaces were probed using an instrumented nanoindentation apparatus (TriboIndenter, Hysitron, Minneapolis, MN) in open-loop feedback mode to five maximum loads corresponding to an indentation contact depth range of approximately 5 nm to 200 nm for both indenter probe radii. This is a rigid load frame, quite distinct in operating principles from the cantilevered loading scheme of an atomic force microscope. Indenters were diamond cones of 60° included angle, terminating in spheres of effective radii R_{eff} = 487 nm and 8724 nm, respectively. The loading profile (2 s loading, 0.5 s unloading) was optimized on the material exhibiting the most creep, PS-12k, according to current nanoindentation analysis theory for viscoelastic materials [22] for the extraction of elastic properties via the Oliver and Pharr method [50]. All tests were conducted at ambient humidity and at 22°C, unless otherwise noted. The load used to define surface contact in open-loop mode was 0.3 μN; however, control experiments were performed using closed-loop mode and indicated that this variation in the initial point detection method does not change the stiffness trend observed for polymer surfaces (data not shown). Humidity controlled experiments were performed on the PS-12k after 4 h of equilibration at each of three conditions: at 42% RH (both before and after the sample was dried in the oven at 105°C for 2 h) and at 10% RH (immediately after oven drying).

Nanoscale mechanical characterization of polymer surfaces includes several experimental factors that can introduce significant error in the estimation of elastic properties [14]. At the outset of this study, these potential artefacts were addressed as follows: root-mean-square surface roughness of CM samples was ≤ 1 nm as prepared; the indentation contact area A_c as a function of contact depth h_c was constructed directly from AFM imaging of the diamond indenter probes, rather than from assumption of ideal spherical geometry corresponding to an effective radius R_{eff}; the loading rate was optimized for the extraction of the reduced elastic modulus E_r [22]; and a sensitivity analysis was conducted to ensure that the observed trends were not affected by the finite contact load preceding acquisition of the load-displacement (P – h) response. Finally, results were quantitatively confirmed by identical experiments on a different instrument (NanoTest600, Micro Materials LLC, Wrexham, UK) for PM-15k with a probe of radius R_{eff} = 3.3 μm.

The apparent stiffness E_a is determined via the reduced elastic modulus E_r, which is a function of a geometrical constant related to the apex angle of the indenter and the indented material Poisson's ratio β, the unloading slope dP/dh at maximum applied load P_{max}, and the maximum projected indentation contact area $A_{max} = A_c$ [50,51].

$$E_r = \beta \frac{dP/dh|_{P_{max}}}{(A_{max})^{1/2}} = \left[\frac{1-\upsilon_i^2}{E_i} + \frac{1-\upsilon_s^2}{E_s}\right]^{-1} \quad (1)$$

where the subscripts i and s denote properties of the indenter and the surface of interest, respectively. Note that E_s is a weak function of the assumed Poisson's ratio of the polymer surface, and that variation of υ_s from 0.1 to 0.4 incurs a change in E_s of less than 10% [52]. Determination of the storage elastic modulus of PS via indenter enabled nanoscale dynamic mechanical analysis (nano-DMA [38,39]) with the probe of radius R_{eff} = 487 nm also indicated quantitatively comparable stiffening over this same range of h_c (Fig. 2d); for any given h_c, the resulting surface areas of contact was greater for the larger probe.

Two conospherical diamond probes with effective radii R_{eff} of 487 nm and 8724 nm were used for nanoindentation. To approximate indenter size, estimates of the effective radii of the two probes were determined by minimizing the error between the area function as predicted by spherical geometry ($A^{sp} = -\pi h_c^2 + 2\pi R_{eff} h_c$) and the numerically computed area. However, for analysis of P – h responses to extract apparent stiffness E_a via Eq. 1, the area function $A_c(h_c)$ was obtained through analysis of AFM image ASCII coordinates (x, y, z) for 1 μm × 1 μm and 5 μm × 5 μm scan sizes. Probes were cleaned with acetone and a lint-free swab before experiments to remove in/organic debris; this was verified through phase images of the probe surface. The contact area as a function of contact depth $A_c(h_c)$ was determined directly via Matlab analysis of AFM tip surface images as motivated and detailed by Van Landingham et al. [23]. Note that determination of E_a from Ac(h_c) is accurate for any body of revolution, even if spherical symmetry is not maintained. The contact surface area of the probes as a function of contact depth was also evaluated via Matlab analysis of AFM tip images by interpolating bilinearly among data points and integrating numerically.

Received: December 13, 2006
Revised: May 15, 2007
Published online: August 17, 2007

[1] C. J. Ellison, J. M. Torkelson, *Nat. Mater.* **2003**, *2*, 695.
[2] J. A. Forrest, K. DalnokiVeress, J. R. Stevens, J. R. Dutcher, *Phys. Rev. Lett.* **1996**, *77*, 2002.
[3] J. L. Keddie, R. A. L. Jones, *Isr. J. Chem.* **1995**, *35*, 21.
[4] K. Akabori, K. Tanaka, T. Nagamura, A. Takahara, T. Kajiyama, *Macromolecules* **2005**, *38*, 9735.
[5] R. D. Priestley, C. J. Ellison, L. J. Broadbelt, J. M. Torkelson, *Science* **2005**, *309*, 456.
[6] M. Alcoutlabi, G. B. McKenna, *J. Phys.: Condens. Matter* **2005**, *17*, R461.
[7] A. Bansal, H. C. Yang, C. Z. Li, K. W. Cho, B. C. Benicewicz, S. K. Kumar, L. S. Schadler, *Nat. Mater.* **2005**, *4*, 693.
[8] C. B. Roth, K. L. McNearny, W. F. Jager, J. M. Torkelson, *Macromolecules* **2007**, *40*, 2568.
[9] T. R. Bohme, J. J. de Pablo, *J. Chem. Phys.* **2002**, *116*, 9939.
[10] K. F. Mansfield, D. N. Theodorou, *Macromolecules* **1991**, *24*, 6283.
[11] R. B. Thompson, V. V. Ginzburg, M. W. Matsen, A. C. Balazs, *Science* **2001**, *292*, 2469.
[12] C. M. Stafford, B. D. Vogt, C. Harrison, D. Julthongpiput, R. Huang, *Macromolecules* **2006**, *39*, 5095.
[13] B. J. Briscoe, K. S. Sebastian, *Proc. R. Soc. London, Ser. A* **1996**, *452*, 439.
[14] M. R. Van Landingham, J. S. Villarrubia, W. F. Guthrie, G. F. Meyers, *Macromol. Symp.* **2001**, *167*, 15.
[15] E. Amitay-Sadovsky, B. Ward, G. A. Somorjai, K. Komvopoulos, *J. Appl. Phys.* **2002**, *91*, 375.
[16] A. Chakravartula, K. Komvopoulos, *Appl. Phys. Lett.* **2006**, *88*, 131901.
[17] H. van Melick, A. van Dijken, J. den Toonder, L. Govaert, H. Meijer, *Philos. Mag. A* **2002**, *82*, 2093.
[18] J. Zhou, K. Komvopoulos, *Appl. Phys. Lett.* **2007**, *90*, 021910.
[19] J. Zhou, K. Komvopoulos, *J. Appl. Phys.* **2006**, *100*, 114329.
[20] J. E. Houston, *J. Polym. Sci., Part B: Polym. Phys.* **2005**, *43*, 2993.
[21] P. Mary, A. Chateauminois, C. Fretigny, *J. Phys. D* **2006**, *39*, 3665.
[22] Y. T. Cheng, C. M. Cheng, *Mater. Sci. Eng. R* **2004**, *44*, 91.
[23] M. R. Van Landingham, T. F. Juliano, M. J. Hagon, *Meas. Sci. Technol.* **2005**, *16*, 2173.
[24] J. A. Forrest, K. Dalnoki-Veress, J. R. Dutcher, *Phys. Rev. E* **1998**, *58*, 6109.

ADVANCED MATERIALS

[25] P. A. O'Connell, G. B. McKenna, *Science* **2005**, *310*, 1431.
[26] P. A. O'Connell, G. B. McKenna, *Eur. Phys. J. E* **2006**, *20*, 143.
[27] C. M. Stafford, C. Harrison, K. L. Beers, A. Karim, E. J. Amis, M. R. Van Landingham, H. C. Kim, W. Volksen, R. D. Miller, E. E. Simonyi, *Nat. Mater.* **2004**, *3*, 545.
[28] C. A. Tweedie, K. J. Van Vliet, *J. Mater. Res.* **2006**, *21*, 1576.
[29] B. J. Briscoe, L. Fiori, E. Pelillo, *J. Phys. D* **1998**, *31*, 2395.
[30] S. Ganguli, D. Dean, K. Jordan, G. Price, R. Vaia, *Polymer* **2003**, *44*, 1315.
[31] R. W. Richards, J. L. Thomason, *Polymer* **1983**, *24*, 1089.
[32] A. Brulet, F. Boue, J. P. Cotton, *J. Phys. II* **1996**, *6*, 885.
[33] J. Bicerano, *Comput. Theor. Polym. Sci.* **1998**, *8*, 9.
[34] D. Yoon, P. Flory, *J. Polym. Phys.* **1976**, *14*, 1425.
[35] P. Rittigstein, J. M. Torkelson, *J. Polym. Sci., Part B: Polym. Phys.* **2006**, *44*, 2935.
[36] R.F. Brady, *Comprehensive Desk Reference of Polymer Characterization and Analysis*, Oxford University Press, Washington, DC **2003**.
[37] a) R. Major, J. Houston, M. McGrath, J. Siepmann, X. Zhu, *Phys. Rev. Lett.* **2006**, *96*, 177 803. b) D.M. Ebenstein, K.J. Wahl, *J. Coll. Interf. Sci.* **2006**, *298*, 652. c) K.J. Wahl, S.A.S. Asif, J.A. Greenwood, K.L. Johnson, *J. Coll. Interf. Sci.* **2006**, *296*, 178. d) K. Mills, X. Zhu, D. Lee, S. Takayama, M. Thouless, *Mater. Res. Soc. Symp. Proc.* **2006**, *924*, 0924-Z07-08. e) M.K. Bernett, W. A. Zisman, *J. Phys. Chem.* **1970**, *74*, 2309.
[38] S. A. S. Asif, K. J. Wahl, R. J. Colton, *Rev. Sci. Instr.* **1999**, *70*, 2408.
[39] S. A. S. Asif, K. J. Wahl, R. J. Colton, O. L. Warren, *J. Appl. Phys.* **2001**, *90*, 1192.
[40] R. A. L. Jones, *Nat. Mater.* **2003**, *2*, 645.
[41] J. Peanasky, L. L. Cai, S. Granick, C. R. Kessel, *Langmuir* **1994**, *10*, 3874.
[42] E. Gacoin, C. Fretigny, A. Chateauminois, A. Perriot, E. Barthel, *Tribol. Lett.* **2006**, *21*, 245.
[43] E. J. Parry, D. Tabor, *J. Mater. Sci.* **1973**, *8*, 1510.
[44] S. A. Hutcheson, G. B. McKenna, *Phys. Rev. Lett.* **2005**, *94*, 076103.
[45] J. S. Sharp, J. H. Teichroeb, J. A. Forrest, *E. Phys. J. E* **2004**, *15*, 473.
[46] A. C. Balazs, T. Emrick, T. P. Russell, *Science* **2006**, *314*, 1107.
[47] A. M. Mayes, *Nat. Mater.* **2005**, *4*, 651.
[48] P. A. Janmey, U. Euteneuer, P. Traub, M. Schliwa, *J. Cell Biol.* **1991**, *113*, 155.
[49] J. Y. Lee, Q. L. Zhang, T. Emrick, A. J. Crosby, *Macromolecules* **2006**, *39*, 7392.
[50] W. C. Oliver, G. M. Pharr, *J. Mater. Res.* **1992**, *7*, 1564.
[51] I. N. Sneddon, *Int. J. Eng. Sci.* **1965**, *3*, 47.
[52] G. Constantinides, K. S. Ravi Chandran, F.-J. Ulm, K. J. Van Vliet, *Mater. Sci. Eng. A* **2006**, *430*, 189.
[53] R. S. Rivlin, *R. Soc. London, Philos. Trans.* **1949**, *242*, 173.
[54] This substrate proximity effect was predicted for $h_c > 20$ nm in these SC films ($t_f = 1140$ nm) from finite element simulations for a Mooney-Rivlin constitutive model [53] polymer film of effective $E = 3.2$ GPa and Poisson's ratio $\upsilon = 0.4$ contacted by a probe of radius $R = 500$ nm (data not shown).
[55] In CM PS-12k, E for $h_c < 50$ nm were statistically greater than those of $h_c > 150$ nm, while only the smallest indentation in CM PM-15k, $h_c \sim 5$ nm, yielded statistically significant increases in E compared to the deepest indentation in that material (statistics via student t-test, $p < 0.05$). To our knowledge, analysis of T_g depression has not been reported for PC. On a non-normalized scale, E of PC ranged ~3.5 to 7 GPa, whereas E of PS ranged from 5.5 to 11 GPa over the same h_c. This comparatively greater compliance of PC is consistent with our own and others' uniaxial measurements of bulk PC and PS, e.g., http://www.matweb.com.
[56] Note that the effective film thicknesses predicted by the model, 125 nm (PS-12k) and 525 nm (PS-197k), correspond to the distance from the free surface over which variation in structural relaxation has also been measured in this polymer[5].